Unique Retrieval of Complex Permittivity and Permeability of Dispersive Materials From Reflection and Transmitted Fields by Enforcing Causality

Vasundara V. Varadan, *Senior Member, IEEE*, and Ruyen Ro, *Member, IEEE*

***Abstract*—The electromagnetic properties of general classes of materials can be obtained by inverting the measured or numerically simulated reflection (S_{11}) and transmission (S_{21}) coefficients through a known thickness of a planar slab of the material. The major difficulty is the uncertainty in the change of phase of the transmitted field, if the phase change exceeds $2m\pi$, $m = 0, 1, 2, \ldots$. This happens for thick samples as well as for highly dispersive materials. An infinite number of solutions are generated for the imaginary part of the complex wavenumber $\gamma = \alpha + j\beta$ for different choices of m. The choice of m can be made unique by noting that for a causal medium, γ is an analytic function of frequency and this results in a Kramers–Kronig-type relation between α and β. Since α is independent of the choice of m and, hence, uniquely determined, a Kramers–Kronig reconstruction of β using α will provide a *guideline* for the correct choice of m. This is a "foolproof" approach even for totally unknown materials since no initial guess is required. Indeed, this approach will work in optics and ultrasonics, and should also be effective for determining the effective refractive index of photonic-bandgap structures that are also highly dispersive.**

***Index Terms*—Dispersive materials, Kramers–Kronig, metamaterials, phase ambiguity, property retrieval, *S*-parameters.**

I. Introduction

PROPAGATION characteristics of electromagnetic (EM) waves in materials can be determined by substituting the corresponding constitutive relations into Maxwell's equations and then solving the dispersion equation. A complete understanding of the EM properties of materials in the frequency range of interest is the basis for the design of materials for RF and microwave applications. There have been several monographs and review papers on microwave methods for materials property characterization [1]–[5]. In the standard transmission line approach (waveguides, coaxial fixtures, focused beam free-space methods), the reflected (S_{11}) and transmitted fields (S_{21}) from a planar finite thickness sample are measured (or numerically simulated) for normal incidence [6]–[9]. For this 1-D wave propagation problem, a constitutive model is adopted for describing the EM response of the sample material and the solution of the EM boundary value problem, leads to two complex equations that relate S_{11} and S_{21} to the constitutive parameters of the sample (Fresnel-type formulas). The use of a vector network analyzer and appropriate calibration techniques permits accurate measurement of both the amplitude and phase of S_{11} and S_{21} and, hence, if the Fresnel formulas involve only two unknown complex material properties, they can be determined in principle.

For an isotropic homogeneous sample, the Nicolson–Ross–Weir algorithm has been widely used for over 30 years [10], [11]. For complex media such as anisotropic materials, chiral materials, or Omega metamaterials, one can follow the solutions to the forward and inverse problems to ascertain what measurement data are necessary and sufficient for unique determination of the constitutive parameters and then develop experimental procedures that are necessary for collecting the needed data [12]–[14]. Although we may have the required data, there is always an ambiguity in determining the change in phase of the transmitted field (S_{21}) because of phase wrapping, if the phase change exceeds 2π, $\phi_{\text{actual}} = \phi_{\text{measured}} + 2m\pi$, $m = 0, 1, 2, \ldots$. For materials described by a complex permittivity and permeability, the Fresnel formulas yields the complex impedance η and the complex wavenumber $\gamma = \alpha + j\beta$. For example, the complex intrinsic impedance η and the attenuation constant α are independent of the phase ambiguity and only the determination of β depends on the phase change [5], [6]. The wavenumber β_m is a function of m and for different values will lie on different Riemann sheets in the complex plane. A detailed description is presented in Section II.

Much work has been done to eliminate the ambiguity in the inverse problem for weakly dispersive media [5], [12]. In such media, it is assumed that the phase velocity ($v_p = \omega/\beta$) does not vary much with frequency and that the group velocity ($v_g = d\omega/d\beta$) is nearly equal to the phase velocity. For example in the group-delay method [6], the calculated phase delay ($\tau_p = d * \beta/\omega$, d is the sample thickness) at each frequency, for each solution of phase constant, is compared with the measured group delay ($\tau_g = -d\phi_{\text{measured}}/d\omega$), which is determined from the slope of the S_{21} *versus* the ω curve. The correct solution for β can be chosen such that the absolute difference between the calculated phase delay and the measured group delay has a minimum value. Another approach is to use samples of two different thicknesses and choose m such that the phase velocity is the same in both samples [15]. In this approach, any uncertainty in sample fabrication may lead to confusion in the selection of the correct solution. This is particularly true for engineered microwave materials such as metamaterials [16], [17].

Manuscript received June 22, 2006; revised October 27, 2006.

The authors are with the Microwave and Optics Laboratory for Imaging and Characterization, Department of Electrical Engineering, University of Arkansas, Fayetteville, AR 72701 USA (e-mail: vvvesm@uark.edu; ryro@isu.edu.tw).

Digital Object Identifier 10.1109/TMTT.2007.906473

For highly dispersive materials such as metamaterials, the response is dominated by plasmonic resonances. The aforementioned approaches may not resolve the phase ambiguity. This is because in regions of anomalous dispersion the transmitted phase has a rapid variation with frequency, and the group velocity can differ greatly from the phase velocity, often becoming larger than the free-space velocity or even negative [18]. It is also mentioned in [16] that group velocity in a region of anomalous dispersion is generally not a useful concept and the approximate definition for the group velocity $v_g = d\omega/d\beta$ is no longer valid. A new "foolproof" approach is needed to resolve the problem of phase ambiguity. In this paper, we enforce causality for the EM response that results in a Kramers–Kronig relationship between α and β. This constraint is used as the basis for a unique inverse algorithm for the retrieval of effective material properties of all types of samples—known, unknown, anisotropic, highly dispersive, etc.

Kramers–Kronig relations are well known in physics. It was initially proposed to relate the real and imaginary parts of the dielectric permittivity for a nonmagnetic material. In optics, especially nonlinear optics, Kramers–Kronig relations have been used to calculate the refractive index of a material by the measurement of the absorbance and they also provide a means to check the self-consistency of experimental or model-generated data [19]–[21]. Recently, we have also applied Kramers–Kronig relations to the effective properties of split-ring resonator metamaterials. The comparison between retrieved properties and calculated data using Kramers–Kronig relations shows a very good agreement. These give us the idea that the constraints between the frequency variation of phase constant β and attenuation constant α can be utilized as a guideline to realize a unique solution to the inverse problem.

II. Application of Kramers–Kronig Relations to the Inverse Problem

The reflection and transmission coefficients S_{11} and S_{21} of a slab sample are employed to retrieve the effective properties, permittivity, and permeability, of the sample. Detailed discussion can be found elsewhere [5], [6], [22]. Only the equations relevant for completeness are included here. From the measured or simulated S_{11} and S_{21}, one can obtain

$$\Gamma = \frac{\eta - \eta_0}{\eta + \eta_0} = K \pm \sqrt{K^2 - 1} \tag{1}$$

with

$$K = \frac{\left(S_{11}^2 - S_{21}^2\right) + 1}{2S_{11}} \tag{2}$$

where Γ is the reflection coefficient at the air–sample interface, and η and η_0 are the impedances for the sample and free space, respectively. The transmission coefficient T is given by

$$T = \exp(-\gamma d) = \frac{(S_{11} + S_{21}) - \Gamma}{1 - (S_{11} + S_{21})\Gamma} \tag{3}$$

where $\gamma = \alpha + j\beta$ is the complex wavenumber, α is the attenuation factor, β is the phase factor, and d is the sample thickness. For a passive medium, the correct choice of the positive or negative sign in (1) is made by the requirement that

$$|\Gamma| \leq 1 \tag{4}$$

or, equivalently,

$$\eta' \geq 0 \tag{5}$$

where η' is the real part of impedance. This ensures that the impedance has a positive resistive part and that the reflected wave amplitude cannot exceed the incident wave amplitude. It follows that the impedance can be uniquely determined as given by

$$\eta = \eta_0 \frac{1 + \Gamma}{1 - \Gamma}. \tag{6}$$

The transmission coefficient T can be obtained from (3). The attenuation and phase factors can then be solved according to

$$\alpha = -\frac{\ln |T|}{d} \tag{7}$$

$$\beta_m = \frac{-\phi_T + 2m\pi}{d} \tag{8}$$

where $|T|$ and ϕ_T are the magnitude and phase of T, respectively, and m is an integer to be determined. It is clear in (7) and (8) that the attenuation factor has a unique solution, whereas β_m has an infinite numbers of solutions. Permittivity ε and permeability μ can be expressed in terms of η and γ as given by

$$\varepsilon = \frac{\gamma}{j\omega\eta} \tag{9}$$

$$\mu = \frac{\gamma\eta}{j\omega} \tag{10}$$

where ω is the angular frequency. The ambiguity in β_m remains and carries over into the determination of ε and μ.

Kramers–Kronig relations are based on the requirement that the response of a material to applied fields should be causal. This then requires that the material parameters describing this response should be analytic functions. Analyticity, in turn, connects the real part of the material properties to an integral containing the corresponding imaginary part and vice versa. Indeed, Kramers–Kronig relations can be formulated for any material property for acoustic, EM, and elastic wave excitation [23]. Here, we apply Kramers–Kronig relations to compute the real part of the complex wavenumber β in terms of the attenuation factor α

$$\frac{\beta_{\text{K-K}}(\omega)}{\beta_0(\omega)} = 1 + \frac{2}{\pi} P \int_0^\infty \frac{\omega' \alpha(\omega')/\beta_0(\omega')}{\omega'^2 - \omega^2} d\omega' \tag{11}$$

where $\beta_0(\omega)$ is the free-space wavenumber and P denotes the principle value of the integral. Note that to compute the value of β accurately in (11), one has to know the value of α as a function of frequency in the entire spectrum. For finite bandwidth data for α, the truncated integration of (11) will cause some error and it

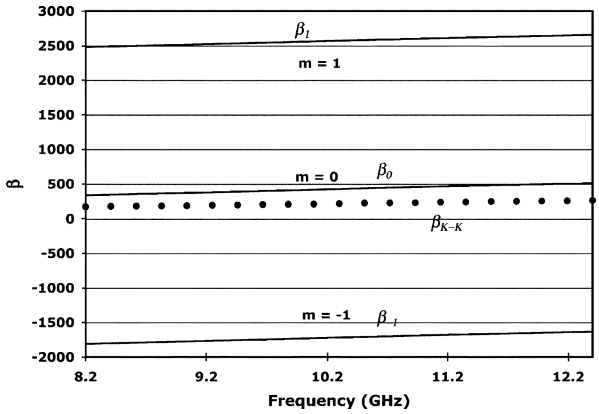

Fig. 1. Phase constants calculated using different values of m for the quartz sample. The values marked with a • are the retrieved phase delay using the Kramers–Kronig relations. The thickness of the quartz sample is 2.93 mm.

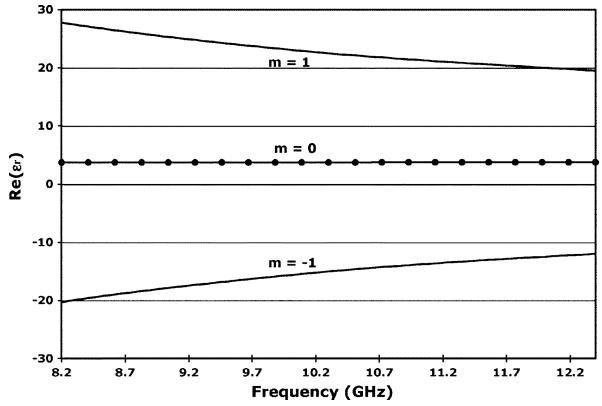

(a)

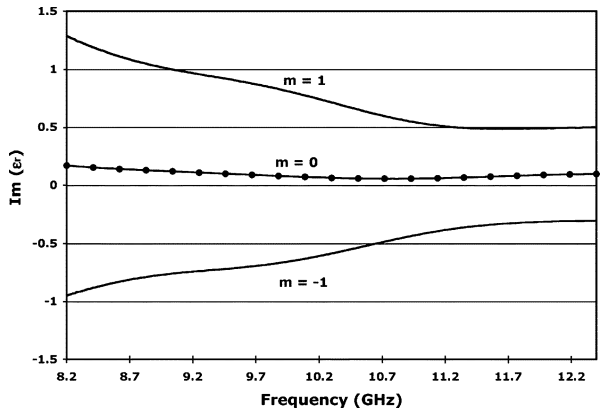

(b)

Fig. 2. (a) $\mathrm{Re}(\varepsilon_r)$, the real part of permittivity calculated using different values of β_m for the quartz sample. $\mathrm{Re}(\varepsilon_r)$ for $m = 0$ is equal to 3.78, denoted by a •, the correct value for quartz. The $m = 0$ value is the one determined using the Kramers–Kronig approach. (b) $\mathrm{Im}(\varepsilon_r)$, the imaginary part of permittivity calculated using different values of β_m for the quartz sample. $\mathrm{Im}(\varepsilon_r)$ for $m = 0$ is nearly 0.07 denoted by a •. The $m = 0$ value is the one determined using the Kramers–Kronig approach.

may become more significant at a band edge [18], [21]. Nevertheless, the retrieved data using Kramers–Kronig relations even for finite bandwidth measurements can yield reasonable agreement with the actual data [21]. The phase factor $\beta_{\text{K-K}}$ using Kramers–Kronig relations will provide a guideline for the correct choice of m in (8). We have applied this approach (hereafter, the Kramers–Kronig approach) to different types of materials such as weakly dispersive media, dispersive media with electrical or magnetic resonance, negative index metamaterial, and magneto-electric media. Some of these results will be illustrated in Section III.

III. Results and Discussion

A computer program comprising (1)–(11) has been developed in our laboratory for the measurement of EM properties in the frequency range of 5–110-GHz range. A simple numerical integration technique, the trapezoidal rule, is employed for calculating $\beta_{\text{K-K}}$ using (11) using α retrieved from (7). In the program, β_m computed for different values of m, as given in (8), are compared with $\beta_{\text{K-K}}$ computed using the Kramers–Kronig relations. The β_m curve that best matches $\beta_{\text{K-K}}$ is chosen as the correct curve for β. In the examples provided here, we can see that the match is unique since only one value of m for a particular frequency range will match with $\beta_{\text{K-K}}$.

Several examples are shown to examine the robustness of the Kramers–Kronig approach to the solution of the inverse problem.

A. Weakly Dispersive Medium

We first consider a thin Quartz sample. In Fig. 1, plots of $\beta_{\text{K-K}}$ and β_m, $m = 0, \pm 1$, in the frequency range of 8.2–12.4 GHz (X-band) are presented. Comparing $\beta_{\text{K-K}}$ and β_m, it is clear in Fig. 1 that $m = 0$ is the appropriate choice. We also observe here that, using finite bandwidth data, the Kramers–Kronig relations cannot be used to calculate the real part of the phase constant using measured imaginary parts. The difference between the actual value of β and $\beta_{\text{K-K}}$ in Fig. 1 is quite significant. The difference can be minimized by using a modified Kramers–Kronig method, as proposed in [19]. For modified methods, we must know the value of β accurately at some region of the spectrum where the material is nondispersive and this constraint can be used to overcome the finite bandwidth data, but that is not of concern here since we are only using the approximate finite bandwidth Kramers–Kronig data to choose the correct β curve from the many possible β_m curves.

The real and imaginary parts of the complex permittivity and permeability (normalized w.r.t. free space) calculating using (9) and (10), respectively, for different values of m are presented in Figs. 2(a) and (b) and 3(a) and (b). For $m = 0$, we correctly obtain $\mathrm{Re}(\varepsilon_r) = 3.78$ and $\mathrm{Re}(\mu_r) = 1$ in the frequency range of interest. The data obtained using $m = 0$, as determined by the Kramers–Kronig approach, and marked with a • in Figs. 2(a) and (b) and 3(a) and (b), give us the correct values for both permittivity and permeability.

B. Dispersive Medium With Magnetic Plasmon Resonance

Here we take the split-ring resonator metamaterial as an example. A detailed description of this sample and the corresponding measurement data can be found in [24]. Note that, for this geometry, the electric field is perpendicular to the gap of the ring so that a symmetric response is observed in the forward and reverse reflection coefficients ($S_{11} = S_{22}$) and,

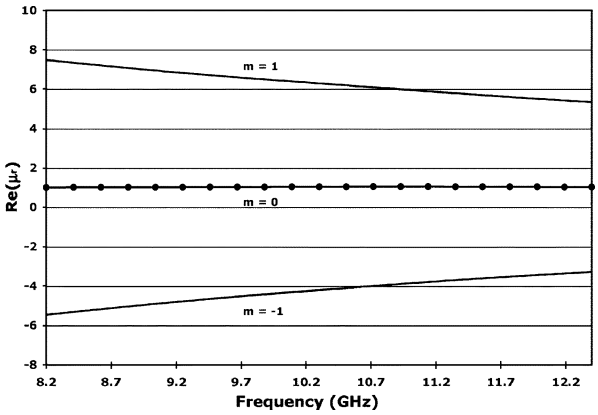

(a)

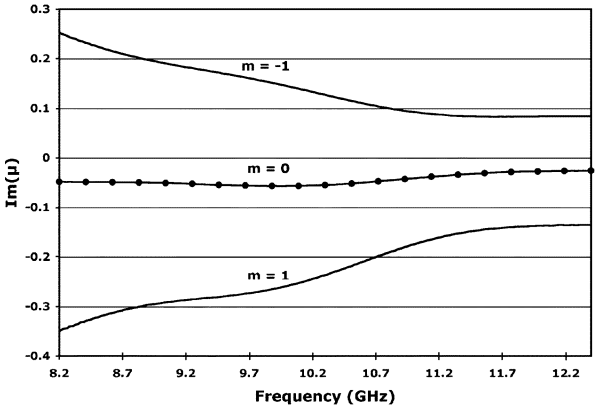

(b)

Fig. 3. (a) $\mathrm{Re}(\mu_r)$, the real part of permeability calculated using different values of β_m for the quartz sample. $\mathrm{Re}(\mu_r)$ for $m = 0$ is equal to 1.0, denoted by a •, the correct value for quartz. The $m = 0$ value is the one determined using the Kramers–Kronig approach. (b) $\mathrm{Im}(\mu_r)$, the imaginary part of permeability calculated using different values of β_m for the quartz sample. $\mathrm{Im}(\mu_r)$ for $m = 0$ is equal to -0.05, denoted by a •, the correct value for quartz. The $m = 0$ value is the one determined using the Kramers–Kronig approach.

hence, the inverse algorithm is still valid. It is shown in [24] that this structure has a magnetic plasmon resonance around 10.4 GHz and in the frequency range above 20 GHz, lattice and plasmonic resonances are also observed.

In Fig. 4, plots of $\beta_{\text{K-K}}$ and β_m, $m = 0, \pm 1$ are presented. From 18.8 to 22 GHz, $\beta d = \pi$, and this results in a bandgap. The value of m varies, with $m = 0$ up to 22 GHz, and then in order to match with $\beta_{\text{K-K}}$ in the frequency ranges of 22.1225–23.6525 and 24.8–26.5 GHz, $m = 1$ yields the correct match, and in the remaining regions, $m = 0$. In these two regions with $m = 1$, the value of βd is slightly greater than π.

Since the range for the phase is from -180° to 180° in the general measurement system, for $\pi \leq \beta d \leq 3\pi$, the measured phase is 2π less than the actual phase and, hence, m being equal to 1 is for the compensation of the phase wrapping. Comparison with $\beta_{\text{K-K}}$ automatically yields the correct phase change.

The retrieved values of the normalized complex permittivity and permeability for different values of m are shown in Figs. 5(a) and (b) and 6(a) and (b). The value of m that agrees with $\beta_{\text{K-K}}$ (with a •) yields the correct values. Around 8.5 GHz, somewhat far away from the magnetic resonance region, the

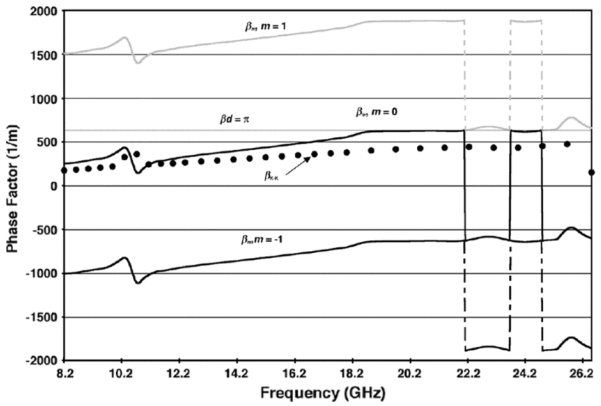

Fig. 4. Real and imaginary parts of the complex wavenumber, $\gamma = \alpha + j\beta$ of the split-ring resonator metamaterial. The thickness of the sample is 5 mm. At resonance, β changes rapidly versus frequency, but the βd value is less than π and, hence, $m = 0$. There is a bandgap from 18.8 to 22 GHz when $\beta d = \pi$, and at 23 GHz, anomalous dispersion will make βd greater than π first and then become less than π, and accordingly, the value of m increases first from 0 to 1 and then decreases from 1 to 0. The $\beta_{\text{K-K}}$ curve remains faithfully close to the variations in m.

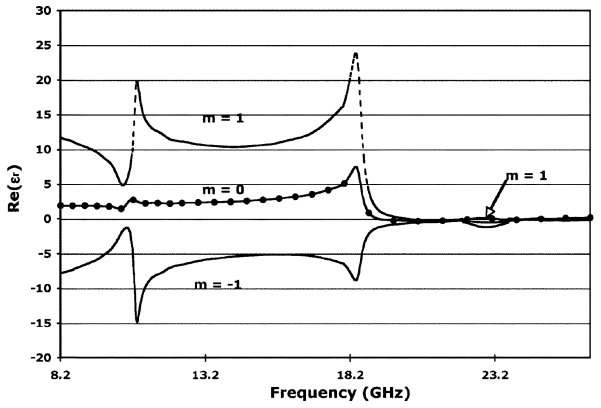

(a)

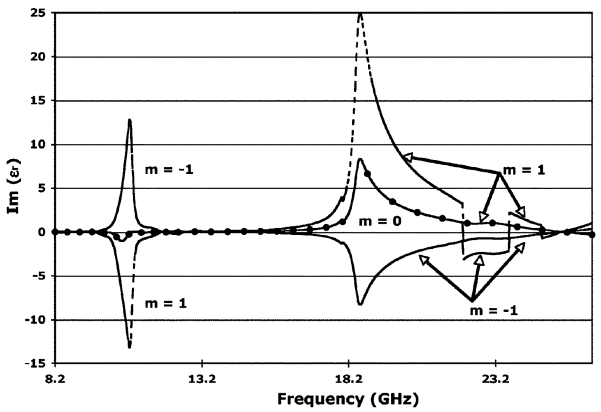

(b)

Fig. 5. (a) $\mathrm{Re}(\varepsilon_r)$, the real part of permittivity for different β_m for the split-ring resonator sample. The values marked with a • for $m = 0$ agree best with the Kramers–Kronig approach. (b) $\mathrm{Im}(\varepsilon_r)$, the imaginary part of permittivity for different β_m for the split-ring resonator sample. The values marked with a • for $m = 0$ agree best with the Kramers–Kronig approach.

real part of permeability obtained using the Kramers–Kronig approach gives a value of 1.08, which shows the split-ring

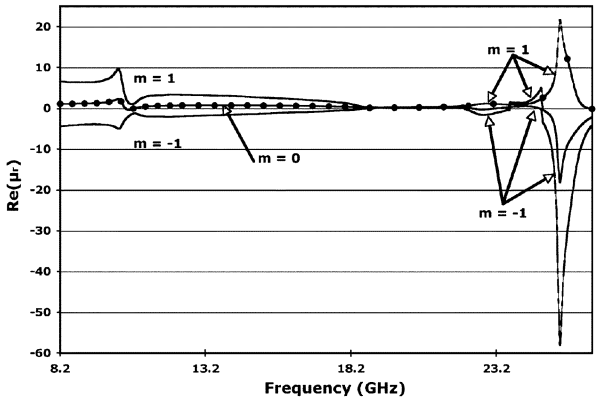

(a)

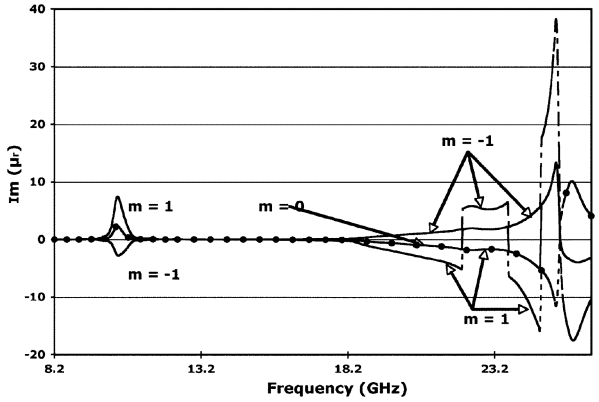

(b)

Fig. 6. (a) $\mathrm{Re}(\mu_r)$, the real part of permeability for different β_m for the split-ring resonator sample. The values marked with a • for $m = 0$ agree best with the Kramers–Kronig approach. (b) $\mathrm{Im}(\mu_r)$, the imaginary part of permeability for different β_m for the split-ring resonator sample. The values marked with a • for $m = 0$ agree best with the Kramers–Kronig approach.

resonator sample is a nonmagnetic material at 8.5 GHz, as it should be. In the region around 10.4 GHz, the complex permittivity and permeability illustrate the traditional resonance and antiresonance phenomena of a magnetic plasmon resonance [24]–[26]. However, there is a clearly defined bandgap when $\beta d = \pi$ when there is no change of β with frequency (slope is $\cong$ zero). After this, the value of m changes many times and it is only comparison of β_m with $\beta_{\text{K-K}}$ that allows us to choose the correct value of m for each frequency range. This is the real utility of using the Kramers–Kronig approach to determine the correct value of the integer m.

C. Drude Medium With Negative Permittivity

The metal wire sample is studied here as an example of a dispersive medium with negative permittivity. The Cu metallization is 0.8-mm wide, 17-μm thick, and printed on dielectric strips 5-mm wide and 0.7-mm thick with $\varepsilon_r = 4 + j0.08$. The strips are arranged in a lattice with a 5-mm period with the E-field parallel to the wires. The attenuation factor α is obtained from the measured S-parameters, as given in (7), $\beta_{\text{K-K}}$ and β_m, $m = 0, \pm 1$, are obtained from (8) and (11) and presented in Fig. 7. The value of m is 0 in the frequency range of 8.2–18 GHz. The retrieved permittivity and permeability are

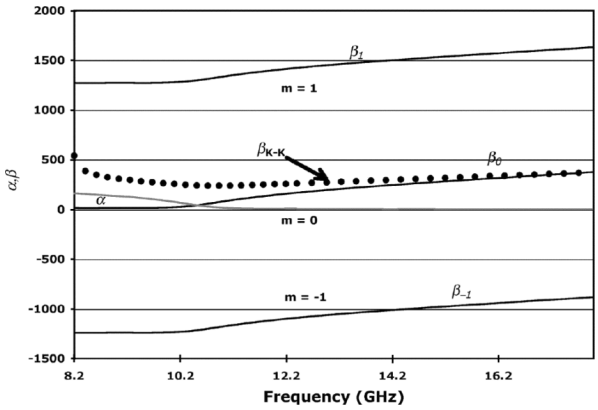

Fig. 7. Real and imaginary parts of the complex wavenumber, $\alpha + j\beta$ of the metal wire sample. The lattice spacing of the wires is 5 mm. Unlike the split-ring resonator sample, attenuation is low even at the Drude frequency of 10.2 GHz The $\beta_{\text{K-K}}$ curve remains faithfully close to the variations in m.

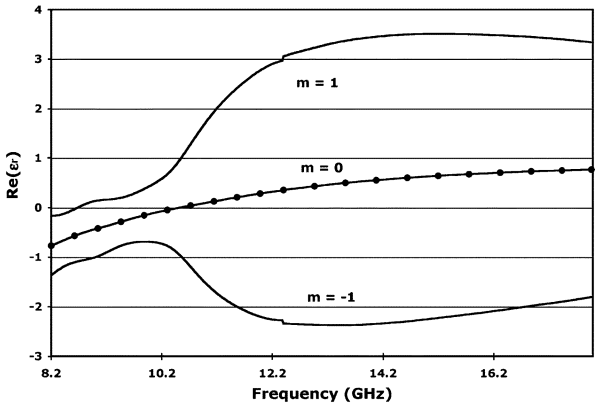

(a)

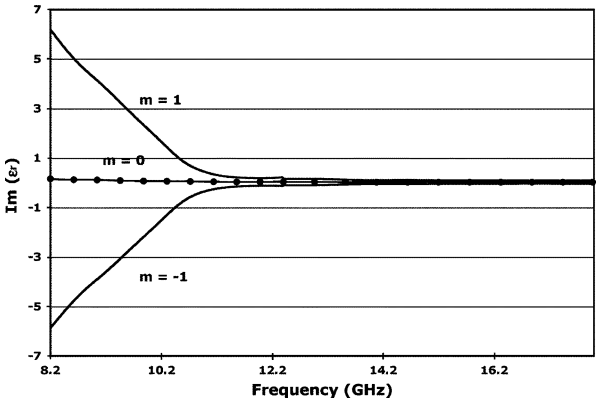

(b)

Fig. 8. (a) $\mathrm{Re}(\varepsilon_r)$, the real part of permittivity calculated for different β_m for the metal wire sample. The values marked with a • for $m = 0$ agree best with the Kramers–Kronig approach. For different values of m, the plasmon (cutoff) frequencies are different, for $m = -1$, $\mathrm{Re}(\varepsilon_r)$ remains negative at all measured frequencies. (b) $\mathrm{Im}(\varepsilon_r)$, the imaginary part of permittivity calculated for different β_m for the metal wire sample. The values marked with a • for $m = 0$ agree best with the Kramers–Kronig approach.

presented in Figs. 8(a) and (b) and 9(a) and (b). The complex permeability using the Kramers–Kronig approach has a real part ranging from 1.14 to 1.3 and a vanishing imaginary part in the frequency range of interest. A Drude model response is

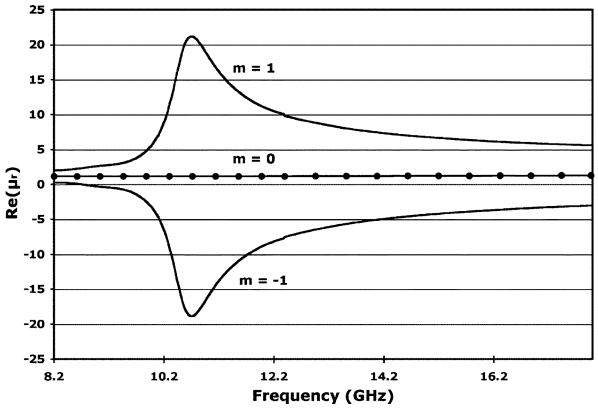

(a)

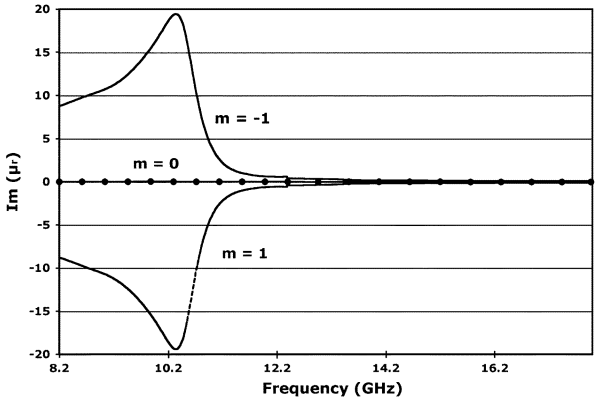

(b)

Fig. 9. (a) $\mathrm{Re}(\mu_r)$, the real part of permeability calculated for different β_m for the metal wire sample. The values marked with a • for $m = 0$ agree best with the Kramers–Kronig approach. (b) $\mathrm{Im}(\mu_r)$, the imaginary part of permeability calculated for different β_m for the metal wire sample. The values marked with a • for $m = 0$ agree best with the Kramers–Kronig approach.

exhibited by the permittivity with a cutoff frequency around 10.5 GHz.

IV. Conclusions

An inverse algorithm with embedded Kramers–Kronig dispersion relations has been presented for the first time to determine a unique solution to the retrieval of material properties from measured S-parameters.

The attenuation factor can be retrieved uniquely from measurement data by the requirement that the real part of impedance cannot be negative. The constraints between the real and imaginary parts of the wavenumber, $\gamma = \alpha + j\beta$ are contained in the Kramers–Kronig relations and employed in this paper to remove the ambiguity in finding β. Measurement results have shown the efficacy and robustness of this approach in retrieving the effective properties of low-loss material and dispersive media described by a Lorentz or Drude model. The phase unwrapping process is automatically implemented in the Kramers–Kronig approach. This implies that our method is a straightforward approach and the only constraint we require is that the medium is causal and passive. This approach we have developed here can also be applied to retrieve the effective properties of nonsymmetric and/or nonreciprocal media and, indeed, will find applications in ultrasonic and optical material property characterization. The method is expected to be particularly useful for highly dispersive systems such as photonic-bandgap (PBG) structures. It is also expected to be useful for characterizing unknown materials where initial guesses cannot be used in an iterative search algorithm.

References

[1] A. R. Von Hippel, Ed., *Dielectric Materials and Applications*. Boston, MA: Artech House, 1995.
[2] E. Nyfors and P. Vainikainen, *Industrial Microwave Sensors*. Norwood, MA: Artech House, 1989.
[3] R. Zoughi, *Microwave Non-Destructive Testing and Evaluation*. Dordrecht, Germany: Kluwer, 2000.
[4] M. U. Afsar, J. R. Birch, R. N. Clarke, and G. W. Chantry, "The measurement of the properties of materials," *Proc. IEEE*, vol. 74, no. 1, pp. 183–199, Jan. 1986.
[5] L. F. Chen, C. K. Ong, C. P. Neo, V. V. Varadan, and V. K. Varadan, *Microwave Electronics: Measurement and Materials Characterization*. West Sussex, U.K.: Wiley, 2004.
[6] D. K. Ghodgaonkar, V. V. Varadan, and V. K. Varadan, "Free-space measurement of complex permittivity and complex permeability of magnetic materials at microwave frequencies," *IEEE Trans. Instrum. Meas.*, vol. 39, no. 2, pp. 387–394, Apr. 1990.
[7] J. Baker-Jarvis, E. J. Vanzura, and W. A. Kissick, "Improved technique for determining complex permittivity with the transmission/reflection method," *IEEE Trans. Microw. Theory Tech.*, vol. 38, no. 8, pp. 1096–1103, Aug. 1990.
[8] W. Barry, "A broadband, automated, stripline technique for the simultaneous measurement of complex permittivity and permeability," *IEEE Trans. Microw. Theory Tech.*, vol. MTT-34, no. 1, pp. 80–84, Jan. 1986.
[9] J. Baker-Jarvis, R. G. Geyer, and P. D. Domich, "A nonlinear least-squares solution with causality constraints applied to transmission line permittivity and permeability determination," *IEEE Trans. Instrum. Meas.*, vol. 41, no. 5, pp. 646–652, Oct. 1992.
[10] A. M. Nicolson and G. F. Ross, "Measurement of the intrinsic properties of materials by time domain techniques," *IEEE Trans. Instrum. Meas.*, vol. IM-19, no. 4, pp. 377–382, Apr. 1970.
[11] W. B. Weir, "Automatic measurement of complex dielectric constant and permeability at microwave frequencies," *Proc. IEEE*, vol. 62, no. 1, pp. 33–36, Jan. 1974.
[12] V. V. Varadan, R. Ro, and V. K. Varadan, "Measurement of the electromagnetic properties of chiral composites in the 8–40 GHz range," *Radio Sci.*, vol. 29, pp. 9–22, 1994.
[13] S. A. Tretyakov and A. A. Sochava, "Novel uniaxial bianisotropic materials: Electromagnetic waves and potential applications," *Electromagnetics*, vol. 9, pp. 157–179, 1994.
[14] I. V. Lindell, M. E. Valtonen, and A. H. Sihvola, "Theory of nonreciprocal and nonsymmetric uniform transmission lines," *IEEE Trans. Microw. Theory Tech.*, vol. 42, no. 2, pp. 291–297, Feb. 1994.
[15] M. Rodriguez-Vidal and E. Martin, "Contribution to numerical methods for calculation of complex dielectric permittivities," *Electron. Lett.*, vol. 6, no. 16, p. 510, 1970.
[16] J. D. Jackson, *Classical Electrodynamics*. New York: Wiley, 1999.
[17] J. B. Pendry, A. J. Holden, W. J. Stewart, and I. Youngs, "Extremely low frequency plasmons in metallic mesostructures," *Phys. Rev. Lett.*, vol. 76, no. 25, pp. 4773–4776, 1996.
[18] J. B. Pendry, A. J. Holden, D. J. Robbins, and W. J. Stewart, "Magnetism from conductors and enhances nonlinear phenomena," *IEEE Trans. Microw. Theory Tech.*, vol. 47, no. 11, pp. 2075–2084, Nov. 1999.
[19] V. Lucarini, J. J. Saarinen, and K.-E. Peiponen, "Multiple subtractive Kramers–Kronig relations for arbitrary-order harmonic generation susceptibilities," *Opt. Commun.*, vol. 218, pp. 409–414, 2003.
[20] K.-E. Peiponen, E. M. Vartiainen, and T. Asakura, *Dispersion, Complex Analysis and Optical Spectroscopy*. Heidelberg, Germany: Springer, 1999.
[21] H. M. Nussenzveig, *Causality and Dispersion Relations*. New York: Academic, 1972.
[22] "Measuring the dielectric constants of solids with the HP8510 network analyzer," Hewlett-Packard, Santa Clara, CA, HP Product Note 8510-3, 1985.
[23] R. L. Weaver and Y.-H. Pao, "Dispersion relations for linear wave propagation in homogeneous and inhomogeneous media," *J. Math. Phys.*, vol. 22, pp. 1909–1918, 1981.

[24] V. V. Varadan and A. R. Tellakula, "Measurement of the complex permittivity, permeability and refractive index in metamaterials composed of discrete split ring resonators in the 8–26 GHz range," *J. Appl. Phys.*, vol. 100, no. 034910, pp. 1–8, 2006.
[25] S. O'Brien and J. B. Pendry, "Magnetic activity at infrared frequencies in structured metallic photonic crystals," *J. Phys., Condens. Matter*, vol. 14, pp. 6383–6394, 2002.
[26] D. R. Smith, S. Schultz, P. Markos, and C. M. Soukoulis, "Determination of effective permittivity and permeability if metamaterials from reflection and transmission coefficients," *Phys. Rev. B, Condens. Matter*, vol. 65, no. 195 104, pp. 1–5, 2002.

Vasundara V. Varadan (M'82–SM'03) received the Ph.D. degree in physics from the University of Illinois at Chicago, in 1974.

She has been with Cornell University, The Ohio State University, and Pennsylvania State University. From 2002 to 2004, she was the Division Director of the Electrical and Communications Systems Division, National Science Foundation (NSF). She is currently the Billingsley Chair and Distinguished Professor of Electrical Engineering with the University of Arkansas, Fayetteville. Her research interests are EM theory and measurements, metamaterials, microwave nondestructive evaluation and imaging, smart materials and devices, numerical simulation of wave problems, and embedded sensor systems.

Dr. Varadan is a Fellow of the Acoustical Society of America, the Institute of Physics (U.K.), and The International Society for Optical Engineers (SPIE). She is an associate editor of the IEEE TRANSACTIONS ON ULTRASONICS, FERROELECTRICS, AND FREQUENCY CONTROL.

Ruyen Ro (M'02) was born in Kaohsiung, Taiwan, R.O.C., in 1959. He received the B.S. degree from National Taiwan University, Taipei, Taiwan, R.O.C., in 1981, and the Ph.D. degree in engineering science from Pennsylvania State University, University Park, in 1991.

In 1991, he joined the Department of Electrical Engineering, I-Shou University, as an Associate Professor, and became a Professor in 1999. In 2002, he was also the Department Head of Communication Engineering, I-Shou University. From 2005 to 2006, he was a Visiting Professor with the University of Arkansas, Fayetteville. His research interests include microwave characterization of complex media, EM theory, surface acoustic-wave devices for communication and sensing applications, and thin-film bulk acoustic wave devices.